BRIEF DEFINITIVE REPORT

Antigen-responsive CD4+ T cell clones contribute to the HIV-1 latent reservoir

Pilar Mendoza[1], Julia R. Jackson[2], Thiago Y. Oliveira[1], Christian Gaebler[1], Victor Ramos[1], Marina Caskey[1], Mila Jankovic[1], Michel C. Nussenzweig[1,3]*, and Lillian B. Cohn[2,4]*

Antiretroviral therapy suppresses but does not cure HIV-1 infection due to the existence of a long-lived reservoir of latently infected cells. The reservoir has an estimated half-life of 44 mo and is largely composed of clones of infected CD4+ T cells. The long half-life appears to result in part from expansion and contraction of infected CD4+ T cell clones. However, the mechanisms that govern this process are poorly understood. To determine whether the clones might result from and be maintained by exposure to antigen, we measured responses of reservoir cells to a small subset of antigens from viruses that produce chronic or recurrent infections. Despite the limited panel of test antigens, clones of antigen-responsive CD4+ T cells containing defective or intact latent proviruses were found in seven of eight individuals studied. Thus, chronic or repeated exposure to antigen may contribute to the longevity of the HIV-1 reservoir by stimulating the clonal expansion of latently infected CD4+ T cells.

Introduction

After integration into the host genome, HIV-1 transcription usually leads to new virus production and cell death. However, HIV-1 can also become latent in a small number of infected CD4+ T cells, and these cells constitute a latent reservoir that is the principle barrier to HIV-1 cure (Bruner and Cohn, 2019). The latent reservoir has a long half-life of ~44 mo (Crooks et al., 2015; Siliciano et al., 2003) and persists in memory CD4+ T cells, including some that are HIV-1, CMV, and influenza specific (Douek et al., 2002; Jones et al., 2012; Demoustier et al., 2002; Hey-Nguyen et al., 2019).

A significant fraction of the circulating latent reservoir is composed of expanded clones of CD4+ T cells containing replication-competent proviruses (≥50%; Bui et al., 2017; Hosmane et al., 2017; Lorenzi et al., 2016; Simonetti et al., 2016; Reeves et al., 2018; Lu et al., 2018; Cohen et al., 2018). Although the origin of the clones and the mechanisms that govern their expansion is not known, longitudinal analysis indicates that they are dynamic and change in size over time in individuals who maintain viral suppression on antiretroviral therapy (ART; Wang et al., 2018; Cohn et al., 2015; Wagner et al., 2014).This dynamic may partially account for the longevity of the reservoir (Bruner and Cohn, 2019). Thus, understanding the basis for latently infected T cell clonal expansion is important for learning how to control and potentially eliminate the reservoir.

HIV-1 proviral DNA is enriched in HIV-1–, CMV-, and influenza-responsive T cells obtained from ART-suppressed individuals, but whether or how this might be related to clonal expansion of T cells harboring latent viruses that remain replication competent has not been examined (Hey-Nguyen et al., 2019; Kristoff et al., 2019; Henrich et al., 2017; Douek et al., 2002; Demoustier et al., 2002; Jones et al., 2012). Here, we report that CD4+ T cells containing clones of replication-competent viruses respond to antigenic stimulation with peptides derived from viruses that cause chronic or recurrent infections.

Results and discussion

To test the hypothesis that expanded clones harboring latent proviruses respond to foreign antigens, we exposed CD4+ T cells from ART-suppressed individuals (Mendoza et al., 2018; Cohen et al., 2018; NCT03571204; Table S1 and Table S2) to overlapping peptide pools from common viral and bacterial antigens including HIV group specific antigen (HIV-gag), CMV phospho-protein 65 (CMV-pp65), or pooled peptides from CMV, EBV, influenza, and tetanus toxin (CEFT). Some of these antigens have been shown to induce HIV-RNA transcription in vivo after vaccination (Stanley et al., 1996; van Sighem et al., 2008). Staphylococcal enterotoxin B (SEB) and a self-protein, myelin oligodendrocyte glycoprotein (MOG), served as positive and negative controls, respectively, for T cell activation. After overnight culture with HIV-gag, CMV-pp65, CEFT, or SEB, activated CD4+ T cells from eight donors were purified by cell

[1]Laboratory of Molecular Immunology, The Rockefeller University, New York, NY;   [2]The Chan Zuckerberg Biohub, San Francisco, CA;   [3]Howard Hughes Medical Institute, The Rockefeller University, New York, NY;   [4]Department of Medicine, University of California, San Francisco, San Francisco, CA.

*M.C. Nussenzweig and L.B. Cohn contributed equally to this paper;   Correspondence to Lillian B. Cohn: lillian.cohn@czbiohub.org;   Michel C. Nussenzweig: nussen@rockefeller.edu.
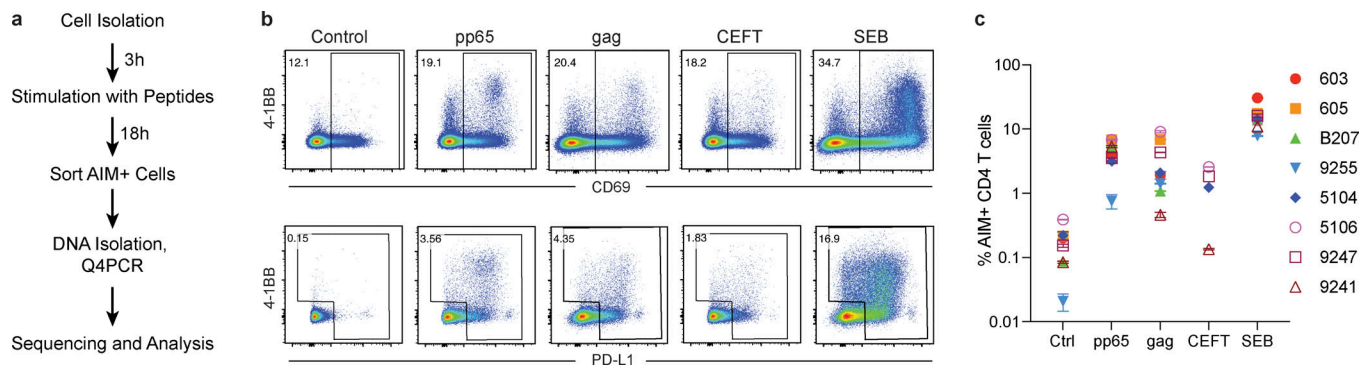
Check for updates

Figure 1. **AIM assay. (a)** Experimental overview. PBMCs were depleted of CD8⁺ T cells and rested for 3 h before stimulation for 18 h with peptide pools. Cells were then purified based on expression of AIMs (CD69, PD-L1, and 4-1BB; Fig. S1). DNA was isolated from sorted cells, Q4PCR was performed, and sequenced viruses were assembled and analyzed. **(b)** Representative example of cell purification by AIM after stimulation with CMV-pp65, HIV-gag, CEFT (from four of eight donors), or SEB by gating on CD69-positive cells followed by gating on PD-L1–positive or 4-1BB–positive cells. Control CD4⁺ T cells cultured with MOG were purified on the basis of CD4 expression alone. Each AIM assay staining was performed twice on each donor (n = 8). Numbers represent the percentage of total CD4⁺ T cells within each gate. **(c)** Frequency of AIM⁺ cells across all donors. Cells were processed and sorted as in panel b.

sorting based on expression of two or more activation-induced markers (AIMs; CD69 and PD-L1 or 4-1BB; Dan et al., 2016; Reiss et al., 2017; Havenar-Daughton et al., 2016; Fig. 1, a and b; and Fig. S1). Total live CD4⁺ T cells were sorted from parallel cultures stimulated with MOG to serve as unfractionated controls that were subjected to the same processing conditions. As expected, there was little detectable response to the MOG self-antigen peptide pool, and all donors showed high-level responses to SEB. In addition, responses to HIV-gag, CMV-pp65, and CEFT varied in magnitude among individuals (Figs. 1 c and S1).

To determine whether CD4⁺ T cells harboring HIV-1 proviruses are enriched among antigen- or SEB-responsive cells compared with the MOG control, integrated proviruses were enumerated and further characterized as intact or defective by combining quantitative PCR (qPCR) and next-generation sequencing (quadraplex qPCR [Q4PCR]; Gaebler et al., 2019; Fig. 2 a). The combination of PCR and sequencing methods enables initial selection of likely-intact viruses by PCR, and these are subsequently confirmed as intact or defective by near-full-length (NFL) proviral amplification and sequencing (Gaebler et al., 2019). As expected, we observed variation in the ratio of intact to defective proviruses between individuals (Ho et al., 2013; Fig. 2 a).

The overall frequency of intact and defective proviruses contained within antigen-responsive cells varied substantially among individuals. For example, proviruses were nearly absent from CMV-pp65–specific CD4⁺ T cells in participant 603 and absent from HIV-gag–specific CD4⁺ T cells in participants 605 or and 5106. In contrast, 1 in 1,000 HIV-gag–responsive cells harbored a provirus in 603 (Fig. 2 and Table S3). Individuals 603 and 9247 showed proviral enrichment in CD4⁺ T cells responding to gag of 2- and 4-fold, respectively, whereas in 605 and 5106, proviruses were 3- and 10-fold enriched in pp65-responsive CD4⁺ T cells (Fig. 2 a). Finally, antigen-responsive cells were relatively depleted of integrated proviruses in participants 9241 and 5104 (Fig. 2 a). We conclude that HIV-1 proviruses can persist in CD4⁺ T cells that respond to CMV-pp65 and HIV-gag antigen with strong variation among infected individuals.

We analyzed all HIV-1 sequences across all groups to determine the fraction of viral sequences contributing to expanded clones of CD4⁺ T cells. Sequences found more than once were classified as derived from clones, while unique sequences were those identified only once. As expected (Bui et al., 2017; Lorenzi et al., 2016; Simonetti et al., 2016; Wang et al., 2018; Cohn et al., 2015, 2018; Maldarelli et al., 2014; Cohen et al., 2018; Lu et al., 2018), clones of viral sequences were identified in all participants (Fig. 2 b). The clonal distribution of HIV-1 sequences in antigen-responsive (HIV-1-gag, CMV-pp65, and CEFT) cells was significantly different from the MOG control in five of the six individuals from whom we were able to obtain >10 sequences (Fig. 2 c). The clonality was not due to T cell division in vitro, as there was no measurable T cell division in 18 h under our culture conditions (Fig. S2). We conclude that cells responding to HIV-gag and CMV-pp65 peptides contain clonal proviruses.

To determine how unique and clonal proviruses contributed to the overall enrichment observed among total HIV-1 sequences, we analyzed the sequences obtained from defective proviruses. Unique sequences were enriched in CMV-pp65–responsive cells from participants 605, 9255, 5104, and 5106 compared with total live CD4⁺ T cells in the MOG control (Fig. 3 a). There was also decreased representation of unique sequences in response to some antigens in 9247 and 9241 (Fig. 3 a). Otherwise, no distinct pattern emerged from the analysis of defective single viruses, and there was no significant antigen-dependent enrichment among unique sequences between the other individuals.

Conversely, compared with total live CD4⁺ T cells in the MOG control, seven of the eight individuals tested showed clones of identical defective proviruses in HIV-gag–, CMV-pp65–, or CEFT-responsive CD4⁺ T cells (Fig. 3 b). The overall enrichment of defective clonal sequences among antigen-responsive cells was often attributable to one or more specific clones. For example, in individuals 603 and 9247, the relative enrichment of defective proviruses corresponds to two clones isolated from HIV-gag–responsive CD4⁺ T cells, whereas two defective clones in 605 and 5104 and four defective clones in B207 account for the HIV-1 enrichment in CMV-pp65–responsive CD4⁺ T cells
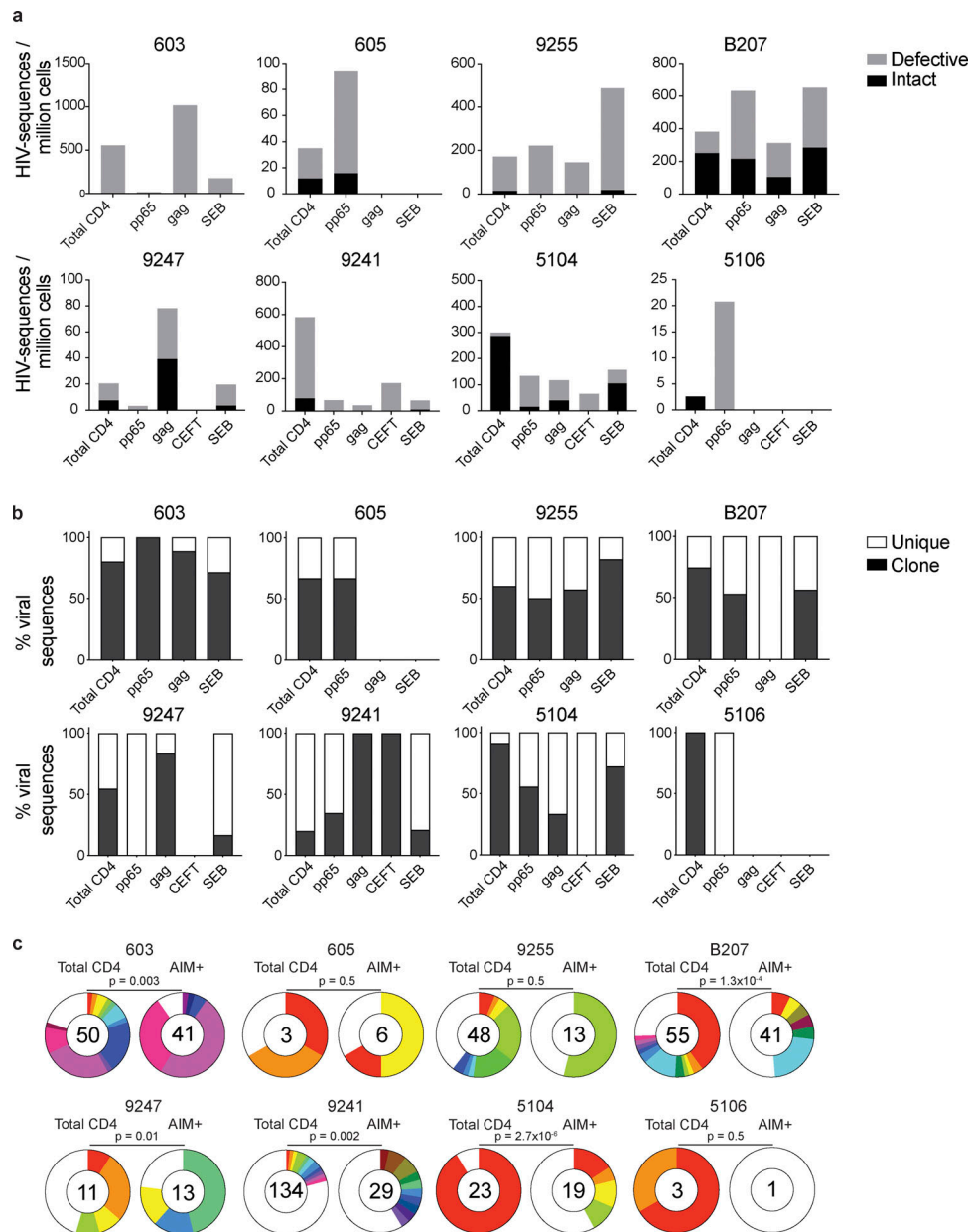
Figure 2. **Defective and intact proviral analysis from antigen-responsive cells. (a)** Frequency of intact (black) and defective (gray) viruses characterized by Q4PCR per million AIM+ CD4+ T cells from eight donors. **(b)** Frequency of virus sequences identified only once (unique) or more than once (clonal) across baseline and all sorted populations from each donor. **(c)** Clonal distribution of Q4PCR-derived HIV-1 sequences from total CD4+ T cells (MOG control) and all antigen-reactive AIM+ CD4+ T cells combined, from eight donors. Numbers in the inner circles indicate the total number of HIV-1 sequences analyzed. White represents sequences identified only once across all conditions (unique), and colored slices represent sequences identified more than once (clones) across baseline and all sorted populations from each donor. The size of each pie slice is proportional to the size of the clone. P values denote a significant change in overall clonal distribution using a two-sided Fisher's exact test. Total DNA extracted from sorted populations was diluted across individual PCR reactions (ranging from 384 to 6,144 reactions) based on gag dilution (see Table S3).

(Fig. 3 b). In addition, participant 9241 showed an enrichment of two proviral clones in CEFT-responsive cells (Fig. 3 b). Because defective viruses cannot infect multiple individual cells, identical defective viruses can arise due to cellular proliferation. We conclude that expanded CD4+ T cell clones harboring defective HIV-1 proviruses are responsive to peptides derived from HIV-gag, CMV-pp65, and CEFT antigens.

SEB is a superantigen that stimulates T cells expressing only a subset of T cell receptors (Llewelyn et al., 2006). Consistent with

this limited specificity, we found that four of the eight individuals tested (9255, B207, 9247, and 5104) had expanded or novel clones of defective proviruses in SEB-reactive CD4+ T cells, compared with the MOG control (Fig. 3 b).

Similar analysis was also performed using intact proviruses, which, as expected, were present in much smaller numbers than defective proviruses (Fig. 4; Ho et al., 2013; Bruner et al., 2016; Hiener et al., 2017; Lu et al., 2018; Gaebler et al., 2019). Unique proviruses were enriched in HIV-gag–specific CD4+ T cells in
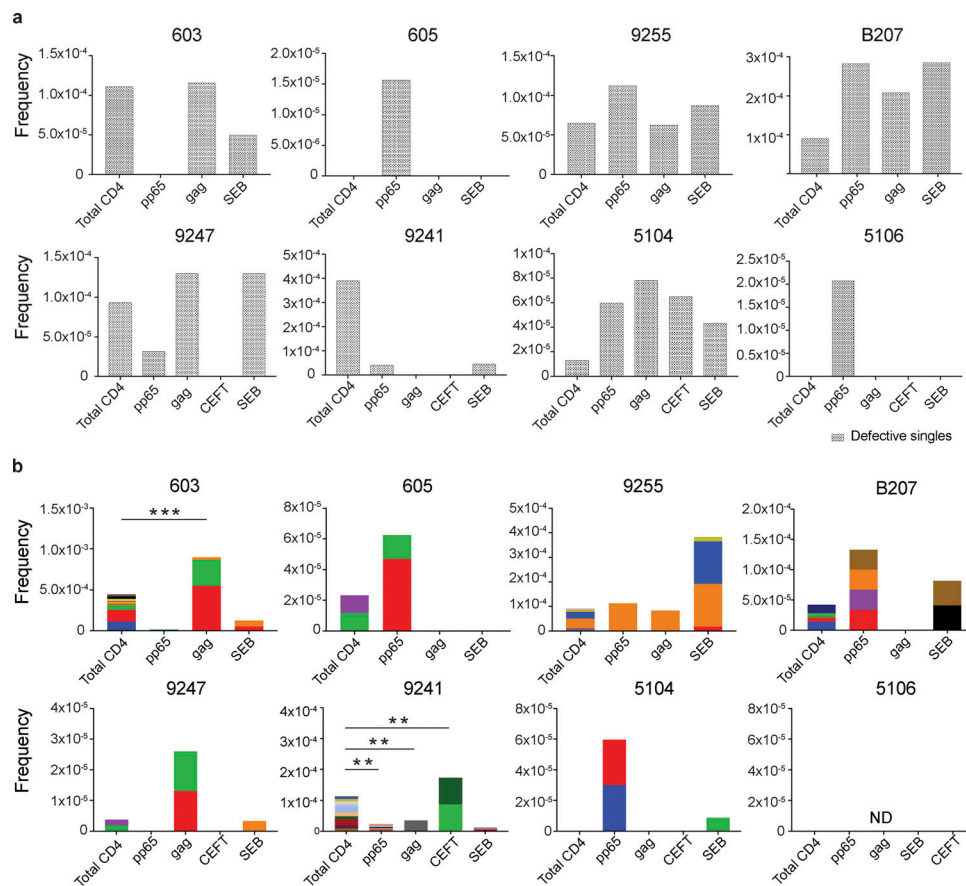
Figure 3. **Defective proviral analysis from antigen-responsive cells. (a)** Frequency of unique defective proviruses isolated from AIM+ cells, calculated by dividing number of sequences by total number of CD4+ T cells analyzed. **(b)** Frequency of clonal defective proviruses isolated from AIM+ cells, calculated by dividing number of clonal sequences by total number of CD4+ T cells analyzed. Each color represents a unique clone. In each donor, clones identified in more than one fraction of cells are represented by the same color. Asterisks denote a significant change in overall clonal distribution (**, P ≤ 0.01; ***, P ≤ 0.001, two-sided Fisher's exact test). Total DNA extracted from sorted populations was diluted across individual PCR reactions (ranging from 384 to 6,144 reactions) based on gag dilution (see Table S3).

participant B207, while in 605, they were found in CMV-pp65–responsive cells (Fig. 4 a).

Antigen- or SEB-responsive CD4+ T cell clones harboring intact proviruses were identified in three and four of the eight participants, respectively (Fig. 4 b). In B207 and 9247, we found clones of CD4+ T cells responding to CMV-pp65 and HIV-gag, respectively. In 9247, this activity was due to a single intact clone of identical proviruses. Although intact proviral clones were found in total CD4+ T cells in the MOG control in participants 9255, 9241, 5104, and 5106, they were nearly entirely absent from antigen-responsive cells (Fig. 4 b). However, the absence of such sequences might be due to the limited number of cells and panel of antigens assayed. We conclude that cells harboring intact proviruses can respond to peptides from HIV-1 and CMV antigens.

To determine whether the intact sequences isolated from antigen-responsive cells are replication competent, we compared the sequences obtained from antigen- or SEB-responsive cells to those obtained from single-cell viral outgrowth cultures (quantitative and qualitative viral outgrowth assay [Q²VOA]) from five of the individuals for whom such data were available (Cohn et al., 2018; Mendoza et al., 2018). We found identical

matches between outgrowth cultures and proviral sequences isolated from either CMV-pp65– or HIV-gag–responsive cells in B207 and 9247 (Fig. 5). Additionally, in participant B207, the intact viruses obtained from the largest CMV-pp65–responsive clone were identical to the clone isolated by latency capture (Cohn et al., 2018). Each member of this clone of CD4+ T cells expressed identical T cell receptor β and α chains (TRBV7-8 and TRAV-21; Cohn et al., 2018). Identical matches for proviruses harbored in SEB-reactive CD4+ T cells were also found in 9255 and B207. Finally, closely related sequences were found in the remaining individuals (Fig. 5). We conclude that clones of CD4+ T cells responsive to HIV-gag, CMV-pp65, and SEB harbor replication-competent viruses.

Understanding the mechanism of latent reservoir persistence is critical to developing methods for HIV-1 eradication or functional cure. We have used a limited number of antigens to test the idea that CD4+ T cells harboring identical latent proviruses can undergo clonal expansion in response to antigenic stimulation. Our results suggest a mechanism for viral persistence whereby clones of infected cells harboring latent proviruses are stimulated to divide during immune responses.

A number of ideas have been proposed to explain HIV-1 persistence. These include low-level ongoing HIV-1 replication
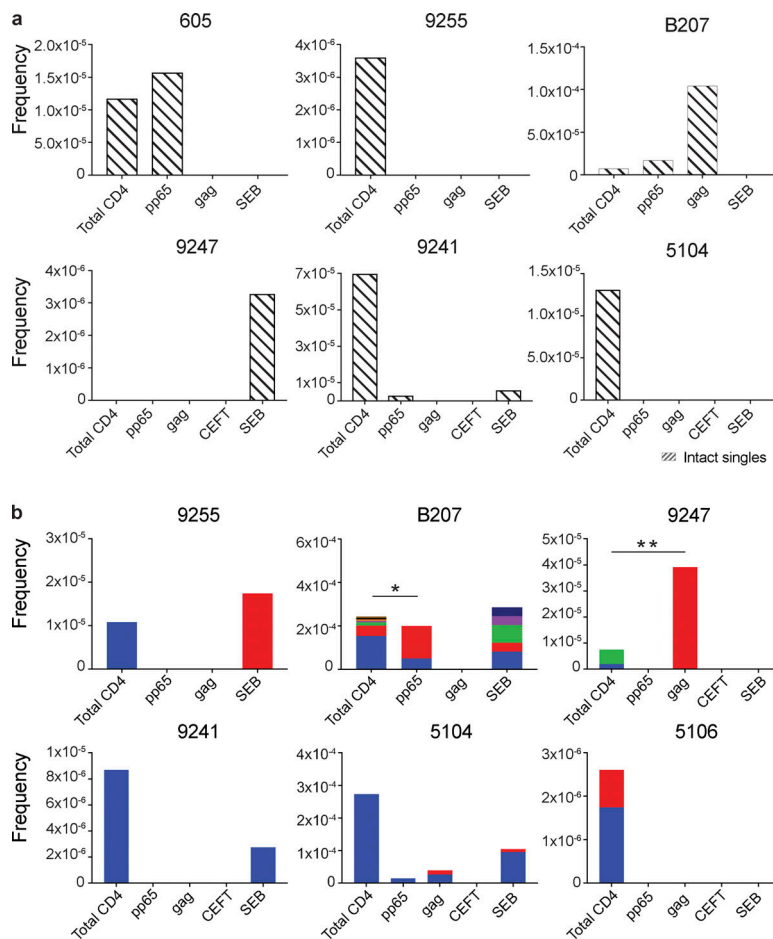
Figure 4. Intact proviral analysis from antigen-responsive cells. (a) Frequency of unique intact proviruses isolated from AIM^{+} cells. **(b)** Frequency of clonal intact proviruses isolated from AIM^{+} cells. Each color represents a unique clone. In each donor, clones identified in more than one fraction of cells are represented by the same color. Asterisks denote a significant change in overall clonal distribution (*, $P \leq 0.05$; **, $P \leq 0.01$, two-sided Fisher's exact test). Total DNA extracted from sorted populations was diluted across individual PCR reactions (ranging from 384 to 6,144 reactions) based on gag dilution (see Table S3).

in sanctuary sites, where drug concentrations are insufficient to block virus replication; and infected T cell longevity (Hatano et al., 2013; Sengupta and Siliciano, 2018). Cell division was not initially considered as a mechanism of proviral persistence because the signals that induce T cell division, such as NF-κB, also tend to reactivate latent proviruses leading to cell death (Siliciano and Greene, 2011). However, several lines of evidence support the idea that CD4^{+} T cells harboring latent proviruses can undergo clonal expansion. Initial indirect support for clonal expansion came from longitudinal human studies showing that ART suppressed individuals produce closely related viruses at low levels over time (Bailey et al., 2006; Tobin et al., 2005). Direct evidence for the existence of expanded clones was obtained from independent cultures of latent CD4^{+} T cells in limiting dilution viral outgrowth assays, suggesting that ≥50% of the circulating reservoir consists of expanded clones (Lorenzi et al., 2016; Hosmane et al., 2017; Bui et al., 2017; Simonetti et al., 2016; Wiegand et al., 2017). In addition, proviral integration site sequencing revealed collections of cells that share identical proviral integration sites (Cohn et al., 2015; Wagner et al., 2014; Maldarelli et al., 2014; McManus et al., 2019). Furthermore, in vitro studies showed that cell division and latency are not mutually exclusive (Wang et al., 2018; Hosmane et al., 2017; Pinzone et al., 2019). Finally, isolation of productively infected cells and paired TCR and full-length viral sequencing (Cohn et al., 2018) and paired full-length viral sequencing and integration site analysis (Einkauf et al., 2019) provided definitive evidence for the existence of expanded clones of CD4^{+} T cells harboring identical intact latent proviruses.

Despite compelling evidence for CD4^{+} T cell proliferation as a mechanism for HIV-1 persistence, how latently infected cells divide without succumbing to cytopathic viral reactivation remains unknown. Possible explanations include expression of genes that favor survival by suppressing viral transcription (Cohn et al., 2018), viral integration in transcriptionally inactive regions of the genome (Craigie and Bushman, 2012), and expression of antiapoptotic proteins such as BIRC5 (Kuo et al., 2018).

Although there is general agreement that a large fraction of the HIV-1 reservoir comprises clones of CD4^{+} T cells that wax and wane (Wang et al., 2018; Lorenzi et al., 2016; Cohen et al., 2018), far less is understood about what triggers clonal expansion and maintains reservoir longevity. It has been proposed that proviral integration in the vicinity of genes that control cell division, such as cancer-associated genes, promotes cell growth (Maldarelli et al., 2014; Wagner et al., 2014). However, HIV-1 is preferentially integrated into highly transcribed genes (Schröder et al., 2002) that include many cancer-associated genes. Thus, it has been difficult to definitively determine whether or how integration in the vicinity of cancer-related genes contributes to HIV-1 persistence (Cohn et al., 2015; Einkauf et al., 2019).
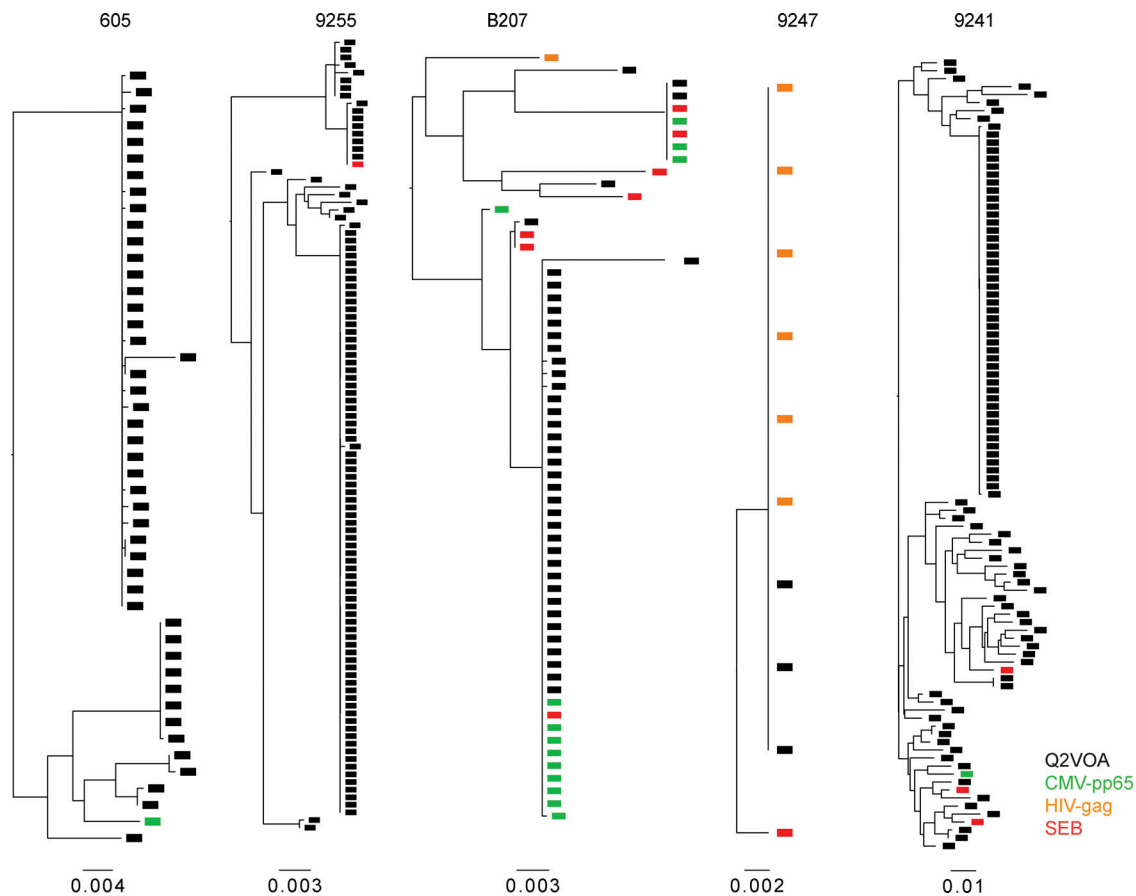
Figure 5. **Phylogenetic tree of *env* sequences.** Maximum likelihood phylogenetic trees of *env* sequences from intact viruses obtained from AIM⁺ cells (green, CMV-pp65; orange, HIV-gag; red, SEB) and Q²VOA single-cell virus outgrowth cultures (black).

Moreover, unlike transforming retroviruses that integrate into cancer genes and cause unrestricted cell growth, HIV-1 is not known to cause T cell cancers by integration.

Our data may provide mechanistic insights into the finding that immunization with tetanus toxoid or influenza can in some, but not all cases, produce increases in HIV-1 RNA in plasma (Christensen-Quick et al., 2018; Stanley et al., 1996). Individuals with vaccine-responsive T cell clones that harbor intact latent viruses would be expected to produce variable amounts of virus after vaccination. The data are also consistent with the report that viral load blips are more frequent during winter months, when there is a higher incidence of seasonal viral infections (van Sighem et al., 2008).

Despite the use of a very limited number of test antigens, our work suggests that expanded clones of CD4⁺ T cells containing replication-competent proviruses respond to pathogens. Their intermittent exposure to these and other antigens found in the virome and microbiome may account for the reported waxing and waning of individual clones of latently infected CD4⁺ T cells and their persistence over time. Finally, barrier tissues that are chronically exposed to antigen, such as the skin or gut, may represent reservoir sites that contribute to persistence of the reservoir by supporting ongoing expansion and contraction of CD4⁺ T cell clones harboring latent proviruses.

Materials and methods

Study design and participants
All study participants were recruited at the Rockefeller University Hospital, New York, NY, and the University Hospital Cologne, Cologne, Germany (Mendoza et al., 2018; Cohen et al., 2018; and https://clinicaltrials.gov/ct2/show/NCT03571204). All participants provided written informed consent before participation in the studies. The studies were conducted in accordance with Good Clinical Practice. The protocols were approved by the institutional review boards at the Rockefeller University and the University of Cologne. Peripheral blood mononuclear cells (PBMCs) were isolated from leukapheresis by Ficoll separation and frozen in aliquots. All participants were confirmed to be aviremic at the time of sample collection. The samples used in the study described here were collected before any investigational therapeutic intervention.

CD4⁺ T cell isolation
Total CD4⁺ T cells from baseline leukapheresis were isolated from cryopreserved PBMCs by manual magnetic labeling and negative selection using the CD4⁺ T Cell Isolation Kit (Miltenyi Biotec).

AIM assay
PBMCs were thawed and washed, and CD8⁺ T cells were depleted using human CD8 MicroBeads (Miltenyi Biotec, 130-045-201).

Mendoza et al.
Antigen-responsive CD4⁺ T cells harbor latent HIV

Journal of Experimental Medicine   6 of 10
https://doi.org/10.1084/jem.20200051

CD8+ T cell–depleted PBMCs were cultured in 24-well plates at a concentration of 10 × 10^6 cells/ml in RPMI 1640 supplemented with Hepes, penicillin/streptomycin, and 10% human serum (Sigma-Aldrich). Cells were rested for 3 h and then stimulated with 0.5 µg/ml of HIV-1 consensus B Gag pool, CMV peptide pool, and CEFT peptide pool (PM-HIV-CONB, PM-PP65-2, PM-CEFT-MHC-II, all from JPT Peptide Technologies) for 18 h at 37°C, 5% CO_2. A MOG peptide pool (0.5 µg/ml, PM-MOG, JPT Peptide Technologies) served as negative control. SEB-stimulated cells (0.5 µg/ml, Toxin Technology, BT202) served as positive control. Cells were stained for viability with Aquavivid (Life Technologies) at 1/200 in PBS for 20 min, 4°C; incubated with human FcR Block (Miltenyi Biotec, 130-059-901) at 1/70 in PBS-FBS 1% for 10 min, 4°C; and stained with antibodies to surface markers for 30 min, 4°C with Brilliant Violet Buffer (BD Biosciences, 566349) at 1/4 in PBS-FBS 1% (see Table S4 for antibody staining panel).

Cell sorting

AIM+ cells were gated on live, single cells, CD14−CD19−CD8−CD4+, and were sorted based on expression of activation markers CD69 and PD-L1 and/or 4-1BB, as previously described (Dan et al., 2016; Reiss et al., 2017; Havenar-Daughton et al., 2016; Niessl et al., 2020). This combination of markers was chosen because of its specificity for activated memory CD4+ T cells with limited background binding by other T cell subsets. MOG- and SEB-treated cells served as negative and positive controls, respectively, to set gates for sorting. MOG-stimulated cells were sorted based on CD14−CD19−CD8−CD4+ expression. CD69 single-positive cells and AIM− cells (CD69−, 4-1BB−, PD-L1−) were also sorted as controls. Cells were sorted on a FACS Aria II flow cytometer (BD Biosciences) into tubes containing RPMI 1640 supplemented with 10% FBS, Hepes and penicillin/streptomycin. Cells were pelleted, and cell pellets were flash frozen on dry ice and subsequently processed for DNA extraction as described below.

Data analysis

Flow cytometric data were analyzed using FlowJo version 10.6.0 for Mac. R programming language was used to apply Fisher's exact test to evaluate whether there was a statistically significant change in the overall distribution of the clones between the Q4PCR-derived HIV-1 sequences from total CD4+ T cells (MOG control) and all antigen-reactive AIM+ CD4+ T cells.

DNA isolation and quantification

Genomic DNA from sorted CD4+ T cells was isolated using phenol-chloroform. Briefly, CD4+ T cells were lysed in proteinase K buffer (100 mM Tris, pH 8, 0.2% SDS, 200 mM NaCl, and 5 mM EDTA) and 20 mg/ml proteinase K at 56°C for 12 h, followed by genomic DNA extraction with phenol/chloroform/isoamyl alcohol (Invitrogen), nonfluorescent pellet paint (Millipore, 70748), and ethanol precipitation. DNA concentration was measured by Qubit High Sensitivity Kit (Thermo Fisher Scientific).

Limiting dilution gag qPCR

To get a measurement of cells containing gag+ proviruses, genomic DNA was serially diluted and assayed by gag qPCR (concentrations ranged from 600 to 12.5 CD4+ T cells per well).

Based on the Poisson distribution, when <30% of qPCR reactions are positive, each positive PCR reaction has a >80% probability of containing a single copy of HIV-1 DNA (Lu et al., 2018). DNA was assayed in a minimum of 16 reactions per concentration in a 384-well plate format using the Applied Biosystem QuantStudio 6 Flex Real-Time PCR System. HIV-1–specific primers and a probe targeting a conserved region in gag were used in a limiting dilution qPCR reaction (forward primer, 5′-ATGTTTTCAGCATTA TCAGAAGGA-3′; internal probe, 5′-6-FAM/CCACCCCAC/ZEN/ AAGATTTAAACACCATGCTAA-3′/IABkFQ; reverse primer, 5′-TGC TTGATGTCCCCCCACT-3′; Integrated DNA Technologies; Palmer et al., 2003).

Each qPCR reaction was performed in a 10-µl total reaction volume containing 5 µl of TaqMan Universal PCR Master Mix containing Rox (4304437; Applied Biosystems), 1 µl of diluted genomic DNA, nuclease-free water, and 337.5 nM of forward and reverse primers with 93.75 nm of gag internal probe. gag qPCR conditions were 94°C for 10 min, 50 cycles of 94°C for 15 s, and 60°C for 60 s.

NFL HIV-1 PCR (NFL1)

We used a two-step nested PCR approach to amplify NFL HIV-1 genomes. All reactions were performed in a 20-µl reaction volume using Platinum Taq High Fidelity polymerase (Thermo Fisher Scientific). The outer PCR reaction (NFL1) was performed on genomic DNA at a single-copy dilution (previously determined by gag limiting dilution) using outer PCR primers BLOuterF (5′-AAATCTCTA GCAGTGGCGCCCGAACAG-3′) and BLOuterR (5′-TGAGGGATCTCT AGTTACCAGAGTC-3′). Touchdown cycling conditions were 94°C for 2 min and then 94°C for 30 s, 64°C for 30 s, and 68°C for 10 min for three cycles; 94°C for 30 s, 61°C for 30 s, and 68°C for 10 min for three cycles; 94°C for 30 s, 58°C for 30 s, and 68°C for 10 min for three cycles; 94°C for 30 s, 55°C for 30 s, and 68°C for 10 min for 41 cycles; and then 68°C for 10 min (Li et al., 2007; Ho et al., 2013).

Q4PCR

Q4PCR was performed as previously described (Gaebler et al., 2019). Briefly, undiluted 1-µl aliquots of the NFL1 PCR product were subjected to a Q4PCR reaction using a combination of four primer/probe sets that target conserved regions in the HIV-1 genome. Each primer/probe set consists of a forward and reverse primer pair as well as a fluorescently labeled internal hydrolysis probe as follows: PS forward, 5′-TCTCTCGACGCA GGACTC-3′; reverse, 5′-TCTAGCCTCCGCTAGTCAAA-3′; probe, 5′-/Cy5/TTTGGCGTA/TAO/CTCACCAGTCGCC-3′/IAbRQSp (Integrated DNA Technologies; Bruner and Siliciano, 2016); env forward, 5′-AGTGGTGCAGAGAGAAAAAAGAGC-3′; reverse, 5′-GTCTGGCCTGTACCGTCAGC-3′; probe, 5′-/VIC/CCTTGGGTTC-TTGGGA-3′/MGB (Thermo Fisher Scientific; Bruner et al., 2016); gag forward, 5′-ATGTTTTCAGCATTATCAGAAGGA-3′; reverse, 5′-TGCTTGATGTCCCCCCACT-3′; probe, 5′-/6-FAM/CCACCCC-AC/ZEN/AAGATTTAAACACCATGCTAA-3′/IABkFQ (Integrated DNA Technologies; Palmer et al., 2003); and pol forward, 5′-GCA CTTTAAATTTTCCCATTAGTCCTA-3′; reverse, 5′-CAAATTTCTACT AATGCTTTTATTTTTTC-3′; probe, 5′-/NED/AAGCCAGGAATGGA-TGGCC-3′/MGB (Thermo Fisher Scientific; Schmid et al., 2010).

Each Q4PCR reaction was performed in a 10-µl total reaction volume containing 5 µl TaqMan Universal PCR Master Mix

Mendoza et al.
Antigen-responsive CD4+ T cells harbor latent HIV

Journal of Experimental Medicine   7 of 10
https://doi.org/10.1084/jem.20200051

containing Rox (4304437; Applied Biosystems), 1 µl diluted genomic DNA, nuclease-free water, and the following primer and probe concentrations: PS, 675 nM of forward and reverse primers with 187.5 nM of PS internal probe; *env*, 90 nM of forward and reverse primers with 25 nM of *env* internal probe; *gag*, 337.5 nM of forward and reverse primers with 93.75 nM of *gag* internal probe; and *pol*, 675 nM of forward and reverse primers with 187.5 nM of *pol* internal probe. qPCR conditions were 94°C for 10 min, 40 cycles of 94°C for 15 s, and 60°C for 60 s. All qPCR reactions were performed in a 384-well plate format using the Applied Biosystem QuantStudio 6 Flex Real-Time PCR System.

qPCR data analysis

We used QuantStudio Real-Time PCR Software version 1.3 (Thermo Fisher Scientific) for data analysis. The same baseline correction (start cycle, 3; end cycle, 10) and normalized reporter signal (ΔRn) threshold (ΔRn threshold = 0.025) was set manually for all targets/probes. Fluorescent signal above the threshold was used to determine the threshold cycle. Samples with a threshold cycle value between 10 and 40 of any probe or probe combination were identified. Samples showing reactivity with two or more of the four qPCR probes were selected for further processing.

Nested NFL HIV-1 PCR (NFL2)

The nested PCR reaction (NFL2) was performed on undiluted 1-µl aliquots of the NFL1 PCR product. Reactions were performed in a 20-µl reaction volume using Platinum Taq High Fidelity polymerase (Thermo Fisher Scientific) and PCR primers 275F (5′-ACAGGGACCTGAAAGCGAAAG-3′) and 280R (5′-CTAGTTACCAGAGTCACACAACAGACG-3′; Ho et al., 2013) at a concentration of 800 nM. Touchdown cycling conditions were 94°C for 2 min and then 94°C for 30 s, 64°C for 30 s, and 68°C for 10 min for three cycles; 94°C for 30 s, 61°C for 30 s, and 68°C for 10 min for three cycles; 94°C for 30 s, 58°C for 30 s, and 68°C for 10 min for three cycles; 94°C for 30 s, 55°C for 30 s, and 68°C for 10 min for 41 cycles; and then 68°C for 10 min.

Library preparation and sequencing

All nested PCR products from NFL2 were subjected to library preparation. The Qubit 3.0 Fluorometer and Qubit dsDNA BR Assay Kit (Thermo Fisher Scientific) were used to measure DNA concentrations. Samples were diluted to a concentration of 10–20 ng/µl. Tagmentation reactions were performed using 1 µl of diluted DNA, 0.25 µl Nextera TDE1 Tagment DNA enzyme (15027865), and 1.25 µl TD Tagment DNA buffer (15027866; Illumina). Tagmented DNA was ligated to unique i5/i7 barcoded primer combinations using the Illumina Nextera XT Index Kit v2 and KAPA HiFi HotStart ReadyMix (2X; KAPA Biosystems) and then purified using AmPure Beads XP (Agencourt). 384 purified samples were pooled into one library and then subjected to paired-end sequencing using Illumina MiSeq Nano 300 V2 cycle kits (Illumina) at a concentration of 12 pM.

HIV-1 sequence assembly and annotation

HIV-1 sequence assembly was performed by our in-house pipeline (Defective and Intact HIV Genome Assembler), which is capable of reconstructing thousands of HIV genomes within hours via the assembly of raw sequencing reads into annotated HIV genomes. The steps executed by the pipeline are described briefly as follows. First, we removed PCR amplification and performed error correction using clumpify.sh from BBtools package v38.72 (https://sourceforge.net/projects/bbmap/). A quality control check was performed with Trim Galore package v0.6.4 (https://github.com/FelixKrueger/TrimGalore) to trim Illumina adapters and low-quality bases. We also used bbduk.sh from BBtools package to remove possible contaminant reads using HIV genome sequences, obtained from Los Alamos HIV database, as a positive control. We used a k-mer–based assembler, SPAdes v3.13.1, to reconstruct the HIV-1 sequences. The longest assembled contig was aligned via BLAST to a database of HIV genome sequences, obtained from Los Alamos, to set the correct orientation. Finally, the HIV genome sequence was annotated by aligning against Hxb2 using BLAST. Sequences with double peaks, i.e., regions indicating the presence of two or more viruses in the sample (cutoff consensus identity for any residue <70%), or samples with a limited number of reads (empty wells ≤500 sequencing reads) were omitted from downstream analyses. In the end, sequences were classified as intact or defective. Defective sequences were subdivided into more specific classifications according to their sequence structure: Major Splice Donor (MSD) Mutation, Non-functional, or Missing Internal Genes.

Clone analysis for intact and defective sequences

Clones were defined by aligning sequences of each classification (Intact, MSD Mutation, Non-functional, and Missing Internal Genes) to HXB2 and calculating their Hamming distance. Sequences having a maximum of three differences between the first nucleotide of gag and the last nucleotide of nef (reference: HXB2) were considered members of the same clone if found more than once across sequences from baseline or all sorted populations (see Cell sorting) retrieved from each participant.

Data availability

All data are available via National Center for Biotechnology Information GenBank under accession nos. MN090896–MN090943 and MT189273–MT191225.

Online supplemental material

Fig. S1 shows the AIM assay flow cytometry plots from all participants. Fig. S2 shows the CFSE proliferation plots after 18 h of stimulation in the AIM assay. Table S1 shows the participants' demographics. Table S2 shows the HLA typing of the study participants. Table S3 shows the gag limiting dilution calculations used for the Q4PCR assay. Table S4 shows the list of antibodies used in flow cytometry for the AIM assay.

Mendoza et al.
Antigen-responsive CD4⁺ T cells harbor latent HIV

Journal of Experimental Medicine   8 of 10
https://doi.org/10.1084/jem.20200051

References

Bailey, J.R., A.R. Sedaghat, T. Kieffer, T. Brennan, P.K. Lee, M. Wind-Rotolo, C.M. Haggerty, A.R. Kamireddi, Y. Liu, J. Lee, et al. 2006. Residual human immunodeficiency virus type 1 viremia in some patients on antiretroviral therapy is dominated by a small number of invariant clones rarely found in circulating CD4+ T cells. J. Virol. 80:6441–6457. https://doi.org/10.1128/JVI.00591-06

Bruner, K.M., and L.B. Cohn. 2019. HIV-1 reservoir dynamics in CD4+ T cells. Curr. Opin. HIV AIDS. 14:108–114. https://doi.org/10.1097/COH.0000000000000521

Bruner, K., and R. Siliciano. 2016. Compositions and methods related to characterizing proviral reservoirs. US patent US20180214473A1, filed by Johns Hopkins University April 22, 2016, pending.

Bruner, K.M., A.J. Murray, R.A. Pollack, M.G. Soliman, S.B. Laskey, A.A. Capoferri, J. Lai, M.C. Strain, S.M. Lada, R. Hoh, et al. 2016. Defective proviruses rapidly accumulate during acute HIV-1 infection. Nat. Med. 22:1043–1049. https://doi.org/10.1038/nm.4156

Bui, J.K., M.D. Sobolewski, B.F. Keele, J. Spindler, A. Musick, A. Wiegand, B.T. Luke, W. Shao, S.H. Hughes, J.M. Coffin, et al. 2017. Proviruses with identical sequences comprise a large fraction of the replication-competent HIV reservoir. PLoS Pathog. 13:e1006283. https://doi.org/10.1371/journal.ppat.1006283

Christensen-Quick, A., A. Chaillon, C. Yek, F. Zanini, P. Jordan, C. Ignacio, G. Caballero, S. Gianella, and D. Smith. 2018. Influenza Vaccination Can Broadly Activate the HIV Reservoir During Antiretroviral Therapy. J. Acquir. Immune Defic. Syndr. 79:e104–e107. https://doi.org/10.1097/QAI.0000000000001829

Cohen, Y.Z., J.C.C. Lorenzi, L. Krassnig, J.P. Barton, L. Burke, J. Pai, C.-L. Lu, P. Mendoza, T.Y. Oliveira, C. Sleckman, et al. 2018. Relationship between latent and rebound viruses in a clinical trial of anti-HIV-1 antibody 3BNC117. J. Exp. Med. 215:2311–2324. https://doi.org/10.1084/jem.20180936

Cohn, L.B., I.T. da Silva, R. Valieris, A.S. Huang, J.C.C. Lorenzi, Y.Z. Cohen, J.A. Pai, A.L. Butler, M. Caskey, M. Jankovic, and M.C. Nussenzweig. 2018. Clonal CD4+ T cells in the HIV-1 latent reservoir display a distinct gene profile upon reactivation. Nat. Med. 24:604–609. https://doi.org/10.1038/s41591-018-0017-7

Cohn, L.B., I.T. Silva, T.Y. Oliveira, R.A. Rosales, E.H. Parrish, G.H. Learn, B.H. Hahn, J.L. Czartoski, M.J. McElrath, C. Lehmann, et al. 2015. HIV-1 integration landscape during latent and active infection. Cell. 160: 420–432. https://doi.org/10.1016/j.cell.2015.01.020

Craigie, R., and F.D. Bushman. 2012. HIV DNA integration. Cold Spring Harb. Perspect. Med. 2:a006890. https://doi.org/10.1101/cshperspect.a006890

Crooks, A.M., R. Bateson, A.B. Cope, N.P. Dahl, M.K. Griggs, J.D. Kuruc, C.L. Gay, J.J. Eron, D.M. Margolis, R.J. Bosch, and N.M. Archin. 2015. Precise Quantitation of the Latent HIV-1 Reservoir: Implications for Eradication Strategies. J. Infect. Dis. 212:1361–1365. https://doi.org/10.1093/infdis/jiv218

Dan, J.M., C.S. Lindestam Arlehamn, D. Weiskopf, R. da Silva Antunes, C. Havenar-Daughton, S.M. Reiss, M. Brigger, M. Bothwell, A. Sette, and S. Crotty. 2016. A Cytokine-Independent Approach To Identify Antigen-Specific Human Germinal Center T Follicular Helper Cells and Rare Antigen-Specific CD4+ T Cells in Blood. J. Immunol. 197:983–993. https://doi.org/10.4049/jimmunol.1600318

Demoustier, A., B. Gubler, M.-G. de Goër, C. Wallon, C. Goujard, J.-F. Delfraissy, and Y. Taoufik. 2002. In patients on prolonged HAART, a significant pool of HIV infected CD4 T cells are HIV-specific. AIDS. 16: 1749–1754. https://doi.org/10.1097/00002030-200209060-00006

Douek, D.C., J.M. Brenchley, M.R. Betts, D.R. Ambrozak, B.J. Hill, Y. Okamoto, J.P. Casazza, J. Kuruppu, K. Kunstman, S. Wolinsky, et al. 2002. HIV preferentially infects HIV-specific CD4+ T cells. Nature. 417:95–98. https://doi.org/10.1038/417095a

Einkauf, K.B., G.Q. Lee, C. Gao, R. Sharaf, X. Sun, S. Hua, S.M.Y. Chen, C. Jiang, X. Lian, F.Z. Chowdhury, et al. 2019. Intact HIV-1 proviruses accumulate at distinct chromosomal positions during prolonged antiretroviral therapy. J. Clin. Invest. 129:988–998. https://doi.org/10.1172/JCI124291

Gaebler, C., J.C.C. Lorenzi, T.Y. Oliveira, L. Nogueira, V. Ramos, C.-L. Lu, J.A. Pai, P. Mendoza, M. Jankovic, M. Caskey, and M.C. Nussenzweig. 2019. Combination of quadruplex qPCR and next-generation sequencing for qualitative and quantitative analysis of the HIV-1 latent reservoir. J. Exp. Med. 216:2253–2264. https://doi.org/10.1084/jem.20190896

Hatano, H., M.C. Strain, R. Scherzer, P. Bacchetti, D. Wentworth, R. Hoh, J.N. Martin, J.M. McCune, J.D. Neaton, R.P. Tracy, et al. 2013. Increase in 2-long terminal repeat circles and decrease in D-dimer after raltegravir intensification in patients with treated HIV infection: a randomized, placebo-controlled trial. J. Infect. Dis. 208:1436–1442. https://doi.org/10.1093/infdis/jit453

Havenar-Daughton, C., S.M. Reiss, D.G. Carnathan, J.E. Wu, K. Kendric, A. Torrents de la Peña, S.P. Kasturi, J.M. Dan, M. Bothwell, R.W. Sanders, et al. 2016. Cytokine-Independent Detection of Antigen-Specific Germinal Center T Follicular Helper Cells in Immunized Nonhuman Primates Using a Live Cell Activation-Induced Marker Technique. J. Immunol. 197:994–1002. https://doi.org/10.4049/jimmunol.1600320

Henrich, T.J., K.S. Hobbs, E. Hanhauser, E. Scully, L.E. Hogan, Y.P. Robles, K.S. Leadabrand, F.M. Marty, C.D. Palmer, J. Sost, et al. 2017. Human Immunodeficiency Virus Type 1 Persistence Following Systemic Chemotherapy for Malignancy. J. Infect. Dis. 216:254–262. https://doi.org/10.1093/infdis/jix265

Hey-Nguyen, W.J., M. Bailey, K. Xu, K. Suzuki, D. Van Bockel, R. Finlayson, A. Leigh Brown, A. Carr, D.A. Cooper, A.D. Kelleher, et al. 2019. HIV-1 DNA Is Maintained in Antigen-Specific CD4+ T Cell Subsets in Patients on Long-Term Antiretroviral Therapy Regardless of Recurrent Antigen Exposure. AIDS Res. Hum. Retroviruses. 35:112–120. https://doi.org/10.1089/aid.2018.0235

Hiener, B., B.A. Horsburgh, J.-S. Eden, K. Barton, T.E. Schlub, E. Lee, S. von Stockenstrom, L. Odevall, J.M. Milush, T. Liegler, et al. 2017. Identification of Genetically Intact HIV-1 Proviruses in Specific CD4+ T Cells from Effectively Treated Participants. Cell Rep. 21:813–822. https://doi.org/10.1016/j.celrep.2017.09.081

Ho, Y.-C., L. Shan, N.N. Hosmane, J. Wang, S.B. Laskey, D.I.S. Rosenbloom, J. Lai, J.N. Blankson, J.D. Siliciano, and R.F. Siliciano. 2013. Replication-competent noninduced proviruses in the latent reservoir increase barrier to HIV-1 cure. *Cell.* 155:540–551. https://doi.org/10.1016/j.cell.2013.09.020

Hosmane, N.N., K.J. Kwon, K.M. Bruner, A.A. Capoferri, S. Beg, D.I.S. Rosenbloom, B.F. Keele, Y.-C. Ho, J.D. Siliciano, and R.F. Siliciano. 2017. Proliferation of latently infected CD4+ T cells carrying replication-competent HIV-1: Potential role in latent reservoir dynamics. *J. Exp. Med.* 214:959–972. https://doi.org/10.1084/jem.20170193

Jones, R.B., C. Kovacs, T.-W. Chun, and M.A. Ostrowski. 2012. Short communication: HIV type 1 accumulates in influenza-specific T cells in subjects receiving seasonal vaccination in the context of effective antiretroviral therapy. *AIDS Res. Hum. Retroviruses.* 28:1687–1692. https://doi.org/10.1089/aid.2012.0115

Kristoff, J., M.L. Palma, T.M. Garcia-Bates, C. Shen, N. Sluis-Cremer, P. Gupta, C.R. Rinaldo, and R.B. Mailliard. 2019. Type 1-programmed dendritic cells drive antigen-specific latency reversal and immune elimination of persistent HIV-1. *EBioMedicine.* 43:295–306. https://doi.org/10.1016/j.ebiom.2019.03.077

Kuo, H.-H., R. Ahmad, G.Q. Lee, C. Gao, H.-R. Chen, Z. Ouyang, M.J. Szucs, D. Kim, A. Tsibris, T.-W. Chun, et al. 2018. Anti-apoptotic Protein BIRC5 Maintains Survival of HIV-1-Infected CD4+ T Cells. *Immunity.* 48:1183–1194.e5. https://doi.org/10.1016/j.immuni.2018.04.004

Li, B., A.D. Gladden, M. Altfeld, J.M. Kaldor, D.A. Cooper, A.D. Kelleher, and T.M. Allen. 2007. Rapid reversion of sequence polymorphisms dominates early human immunodeficiency virus type 1 evolution. *J. Virol.* 81:193–201. https://doi.org/10.1128/JVI.01231-06

Llewelyn, M., S. Sriskandan, N. Terrazzini, J. Cohen, and D.M. Altmann. 2006. The TCR Vbeta signature of bacterial superantigens spreads with stimulus strength. *Int. Immunol.* 18:1433–1441. https://doi.org/10.1093/intimm/dxl076

Lorenzi, J.C.C., Y.Z. Cohen, L.B. Cohn, E.F. Kreider, J.P. Barton, G.H. Learn, T. Oliveira, C.L. Lavine, J.A. Horwitz, A. Settler, et al. 2016. Paired quantitative and qualitative assessment of the replication-competent HIV-1 reservoir and comparison with integrated proviral DNA. *Proc. Natl. Acad. Sci. USA.* 113:E7908–E7916. https://doi.org/10.1073/pnas.1617789113

Lu, C.-L., J.A. Pai, L. Nogueira, P. Mendoza, H. Gruell, T.Y. Oliveira, J. Barton, J.C.C. Lorenzi, Y.Z. Cohen, L.B. Cohn, et al. 2018. Relationship between intact HIV-1 proviruses in circulating CD4+ T cells and rebound viruses emerging during treatment interruption. *Proc. Natl. Acad. Sci. USA.* 115:E11341–E11348. https://doi.org/10.1073/pnas.1813512115

Maldarelli, F., X. Wu, L. Su, F.R. Simonetti, W. Shao, S. Hill, J. Spindler, A.L. Ferris, J.W. Mellors, M.F. Kearney, et al. 2014. HIV latency. Specific HIV integration sites are linked to clonal expansion and persistence of infected cells. *Science.* 345:179–183. https://doi.org/10.1126/science.1254194

McManus, W.R., M.J. Bale, J. Spindler, A. Wiegand, A. Musick, S.C. Patro, M.D. Sobolewski, V.K. Musick, E.M. Anderson, J.C. Cyktor, et al. 2019. HIV-1 in lymph nodes is maintained by cellular proliferation during antiretroviral therapy. *J. Clin. Invest.* 130:4629–4642. https://doi.org/10.1172/JCI126714

Mendoza, P., H. Gruell, L. Nogueira, J.A. Pai, A.L. Butler, K. Millard, C. Lehmann, I. Suárez, T.Y. Oliveira, J.C.C. Lorenzi, et al. 2018. Combination therapy with anti-HIV-1 antibodies maintains viral suppression. *Nature.* 561:479–484. https://doi.org/10.1038/s41586-018-0531-2

Niessl, J., A.E. Baxter, P. Mendoza, M. Jankovic, Y.Z. Cohen, A.L. Butler, C.-L. Lu, M. Dubé, I. Shimeliovich, H. Gruell, et al. 2020. Combination anti-HIV-1 antibody therapy is associated with increased virus-specific T cell immunity. *Nat. Med.* 26:222–227. https://doi.org/10.1038/s41591-019-0747-1

Palmer, S., A.P. Wiegand, F. Maldarelli, H. Bazmi, J.M. Mican, M. Polis, R.L. Dewar, A. Planta, S. Liu, J.A. Metcalf, et al. 2003. New real-time reverse transcriptase-initiated PCR assay with single-copy sensitivity for human immunodeficiency virus type 1 RNA in plasma. *J. Clin. Microbiol.* 41:4531–4536. https://doi.org/10.1128/JCM.41.10.4531-4536.2003

Pinzone, M.R., D.J. VanBelzen, S. Weissman, M.P. Bertuccio, L. Cannon, E. Venanzi-Rullo, S. Migueles, R.B. Jones, T. Mota, S.B. Joseph, et al. 2019. Longitudinal HIV sequencing reveals reservoir expression leading to decay which is obscured by clonal expansion. *Nat. Commun.* 10:728. https://doi.org/10.1038/s41467-019-08431-7

Reeves, D.B., E.R. Duke, T.A. Wagner, S.E. Palmer, A.M. Spivak, and J.T. Schiffer. 2018. A majority of HIV persistence during antiretroviral therapy is due to infected cell proliferation. *Nat. Commun.* 9:4811. https://doi.org/10.1038/s41467-018-06843-5

Reiss, S., A.E. Baxter, K.M. Cirelli, J.M. Dan, A. Morou, A. Daigneault, N. Brassard, G. Silvestri, J.-P. Routy, C. Havenar-Daughton, et al. 2017. Comparative analysis of activation induced marker (AIM) assays for sensitive identification of antigen-specific CD4 T cells. *PLoS One.* 12:e0186998. https://doi.org/10.1371/journal.pone.0186998

Schmid, A., S. Gianella, V. von Wyl, K.J. Metzner, A.U. Scherrer, B. Niederöst, C.F. Althaus, P. Rieder, C. Grube, B. Joos, et al. 2010. Profound depletion of HIV-1 transcription in patients initiating antiretroviral therapy during acute infection. *PLoS One.* 5:e13310. https://doi.org/10.1371/journal.pone.0013310

Schröder, A.R.W., P. Shinn, H. Chen, C. Berry, J.R. Ecker, and F. Bushman. 2002. HIV-1 integration in the human genome favors active genes and local hotspots. *Cell.* 110:521–529. https://doi.org/10.1016/S0092-8674(02)00864-4

Sengupta, S., and R.F. Siliciano. 2018. Targeting the Latent Reservoir for HIV-1. *Immunity.* 48:872–895. https://doi.org/10.1016/j.immuni.2018.04.030

Siliciano, J.D., J. Kajdas, D. Finzi, T.C. Quinn, K. Chadwick, J.B. Margolick, C. Kovacs, S.J. Gange, and R.F. Siliciano. 2003. Long-term follow-up studies confirm the stability of the latent reservoir for HIV-1 in resting CD4+ T cells. *Nat. Med.* 9:727–728. https://doi.org/10.1038/nm880

van Sighem, A., S. Zhang, P. Reiss, L. Gras, M. van der Ende, F. Kroon, J. Prins, and F. de Wolf. 2008. Immunologic, virologic, and clinical consequences of episodes of transient viremia during suppressive combination antiretroviral therapy. *J. Acquir. Immune Defic. Syndr*. 48(1):104–108. https://doi.org/10.1097/QAI.0b013e31816a1d4f

Siliciano, R.F., and W.C. Greene. 2011. HIV latency. *Cold Spring Harb. Perspect. Med.* 1:a007096. https://doi.org/10.1101/cshperspect.a007096

Simonetti, F.R., M.D. Sobolewski, E. Fyne, W. Shao, J. Spindler, J. Hattori, E.M. Anderson, S.A. Watters, S. Hill, X. Wu, et al. 2016. Clonally expanded CD4+ T cells can produce infectious HIV-1 in vivo. *Proc. Natl. Acad. Sci. USA.* 113:1883–1888. https://doi.org/10.1073/pnas.1522675113

Stanley, S.K., M.A. Ostrowski, J.S. Justement, K. Gantt, S. Hedayati, M. Mannix, K. Roche, D.J. Schwartzentruber, C.H. Fox, and A.S. Fauci. 1996. Effect of immunization with a common recall antigen on viral expression in patients infected with human immunodeficiency virus type 1. *N. Engl. J. Med.* 334:1222–1230. https://doi.org/10.1056/NEJM199605093341903

Tobin, N.H., G.H. Learn, S.E. Holte, Y. Wang, A.J. Melvin, J.L. McKernan, D.M. Pawluk, K.M. Mohan, P.F. Lewis, J.I. Mullins, and L.M. Frenkel. 2005. Evidence that low-level viremias during effective highly active antiretroviral therapy result from two processes: expression of archival virus and replication of virus. *J. Virol.* 79:9625–9634. https://doi.org/10.1128/JVI.79.15.9625-9634.2005

Wagner, T.A., S. McLaughlin, K. Garg, C.Y.K. Cheung, B.B. Larsen, S. Styrchak, H.C. Huang, P.T. Edlefsen, J.I. Mullins, and L.M. Frenkel. 2014. HIV latency. Proliferation of cells with HIV integrated into cancer genes contributes to persistent infection. *Science.* 345:570–573. https://doi.org/10.1126/science.1256304

Wang, Z., E.E. Gurule, T.P. Brennan, J.M. Gerold, K.J. Kwon, N.N. Hosmane, M.R. Kumar, S.A. Beg, A.A. Capoferri, S.C. Ray, et al. 2018. Expanded cellular clones carrying replication-competent HIV-1 persist, wax, and wane. *Proc. Natl. Acad. Sci. USA.* 115:E2575–E2584. https://doi.org/10.1073/pnas.1720665115

Wiegand, A., J. Spindler, F.F. Hong, W. Shao, J.C. Cyktor, A.R. Cillo, E.K. Halvas, J.M. Coffin, J.W. Mellors, and M.F. Kearney. 2017. Single-cell analysis of HIV-1 transcriptional activity reveals expression of proviruses in expanded clones during ART. *Proc. Natl. Acad. Sci. USA.* 114:E3659–E3668. https://doi.org/10.1073/pnas.1617961114
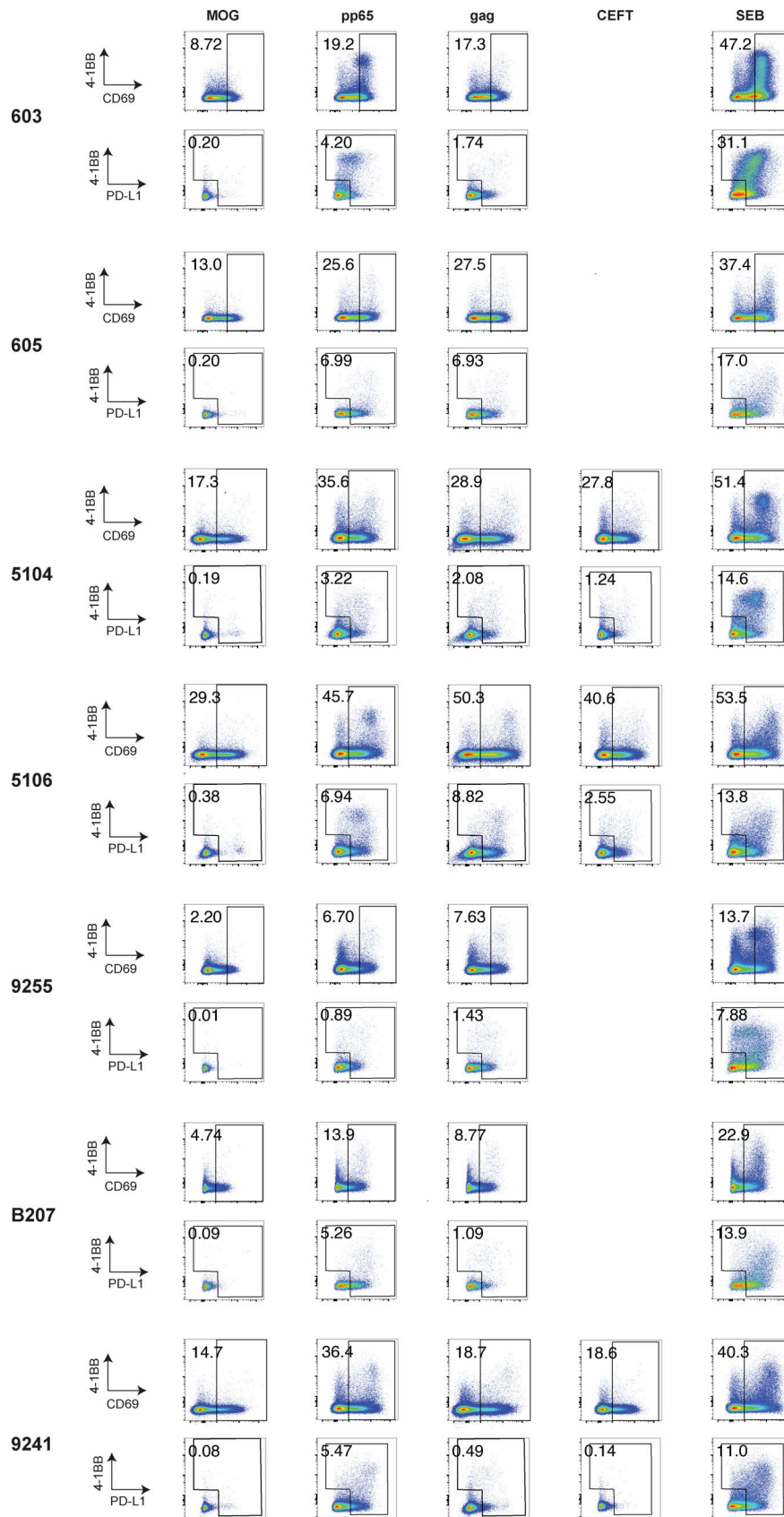
Figure S1. AIM flow cytometry plots. CD4+ T cells were stimulated for 18 h with peptide pools from MOG (control), CMV-pp65, HIV-gag, CEFT, or SEB before staining. CD4+ T cells were gated on CD69-positive cells, followed by gating on PD-L1–positive and/or 4-1BB–positive cells. Each AIM assay staining was performed twice on each donor. Numbers represent the percentage of total CD4+ T cells within each gate.
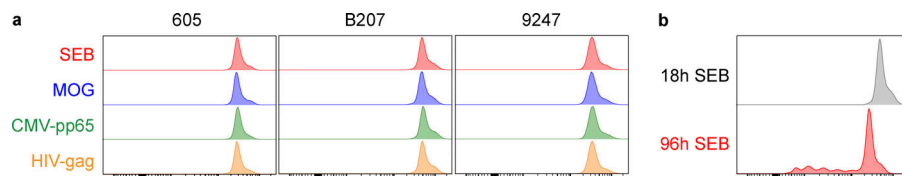
Figure S2. **CFSE proliferation assay after 18-h stimulation. (a)** CFSE-labeled CD4$^+$ T cells from participants 605, B207, and 9247 were stimulated with peptide pools from MOG (control), CMV-pp65, HIV-gag, or SEB before staining. Histograms show CFSE labeling of CD4$^+$ T cells after 18 h of stimulation. **(b)** Representative histograms of CFSE labeling within CD4$^+$ T cells for participant B207 after 18 and 96 h of stimulation with SEB, respectively. Each AIM assay staining was performed twice on each donor.

Tables S1–S4 are provided online as separate Word files. Table S1 shows donor characteristics. Table S2 shows donor HLA genotyping. Table S3 shows HIV-1 gag DNA enrichment in the different sorted populations. Table S4 lists antibodies used in flow cytometry for cell sorting and identification of antigen-reactive cells.